



POLITECNICO
MILANO 1863

[RE.PUBLIC@POLIMI](#)

Research Publications at Politecnico di Milano

Post-Print

This is the accepted version of:

S. Dossi, F. Maggi

Ignition of Mechanically Activated Aluminum Powders Doped with Metal Oxides
Propellants, Explosives, Pyrotechnics, Vol. 44, N. 10, 2019, p. 1312-1318
doi:10.1002/prop.201900036

The final publication is available at <https://doi.org/10.1002/prop.201900036>

Access to the published version may require subscription.

This is the peer reviewed version of the following article: Ignition of Mechanically Activated Aluminum Powders Doped with Metal Oxides, which has been published in final form at <https://doi.org/10.1002/prop.201900036>. This article may be used for non-commercial purposes in accordance with Wiley Terms and Conditions for Use of Self-Archived Versions.

When citing this work, cite the original published paper.

Permanent link to this version

<http://hdl.handle.net/11311/1100716>

Ignition of Mechanically Activated Aluminum Powders Doped with Metal Oxides

Stefano Dossi,^{[a],[b]} Filippo Maggi*^[c]

Abstract: Use of mechanical milling to increase micrometric powder reactivity is of interest due to several intrinsic advantages of this technique (e.g. versatility and safety). In this work, 30 μm propulsion-grade aluminum has been activated with and without metal oxides. The powders so obtained were characterized in terms of particle size distribution, metal content, morphology, and ignition temperature. This last parameter represents a good indicator to rate the reaction properties of powders and the effects of activation parameters on the final product. All the ingredients containing metal oxides feature an enhanced reactivity as a consequence of both additives and modification of particle morphology.

Keywords: activated aluminum, ball milling, ignition temperature, reactivity enhancement

1 Introduction

Solid rocket motors (SRMs) derive different kinds of benefits from the introduction of metal powders in the composition of their energetic material (e.g., improved gravimetric specific impulse, augmented energy density or damping of combustion instabilities). In this field, the most used substance is micrometric aluminum (μAl) in the form of 15-30 μm spherical particles. Despite an interesting series of advantages (e.g. relatively low toxicity, high combustion enthalpy, availability, and low cost), μAl suffers from difficult ignition and relatively slow burning leading part of the metal to aggregate at the burning surface and finally to generate droplets of molten metal (aggregation-to-agglomeration process) [1]. The presence of a two-phase flow expanding through the nozzle causes a reduction of delivered performance depending on the average condensed combustion product (CCP) size, and quantified in about 3-4% of the ideal gravimetric specific impulse [2]. Reduction of agglomerate dimension is then a key-factor to recover part of the performance losses in SRMs. A leading role in CCP size reduction can be played by innovative metal fuels having a higher reactivity with respect to μAl such as nano-aluminum (nAl) and activated aluminum (aAl).

Nanometric aluminum is a very reactive

material characterized by a high specific surface area and low ignition temperature [3]. Several studies carried out by DeLuca et al. [4,5] and Maggi et al. [6] have proven that the use of nAl instead of μAl strongly modifies the aggregation-to-agglomeration processes occurring on the propellant burning surface. In presence of the nano-metal, a fraction of the particles tend to group and enter the gas phase in flake-kind structures, instead of molten spherical drops. A strong reduction of CCP size was observed after quenching and collection of residues. These metal powders manifest enhanced reactivity, assuring an increment of the SP burning rate [7]. Aluminum powders are naturally coated by a thin layer of oxide that has been evaluated in the range of about 3-5 nm [8-11]. According to literature evidences, its thickness is repeatedly independent of particle size. Therefore, the active metal content of Al powders decreases progressively when particles tend to become nanometric, reducing the actual specific impulse of a related aluminized propellant. This fact may partially or totally annihilate the advantages connected with the reactivity increment. Thermochemical calculations revealed that a reduction of 15% of the Al content is sufficient to jeopardize the performance gain obtainable by eliminating the agglomeration phenomenon [8]. Moreover, the high specific surface area of nAl can introduce manufacturing issues due to the increment of mixing viscosity. [10, 12].

A different strategy to increase powder reactivity is μAl activation. The process aims at obtaining a compromise between nano- and micro-powders, with the possibility of producing *ad-hoc* materials. The powder is kept micrometric so it preserves a higher metal content with respect to nano-particles, contemporarily reducing manufacturing problems [8, 13]. Activation processes can be realized chemically, e.g. using fluorinated substances, mechanically by grinding powders with high energy mills, or mechanochemically, e.g. alloying two or more metals to produce intermetallic species or to change the structure of the original material. In the first case, the chemical processing aims at weakening the Al oxide layer, facilitating metal oxidation [14]. However,

[a] S. Dossi
ReActive - Powder Technology
Via Durando 38A, 20156 Milan, Italy
E-mail: stefano.dossi@reactivepowders.com

[b] S. Dossi
Dept. Aerospace Science and Technology
Politecnico di Milano
Via La Masa 34, 20156 Milano, Italy
E-mail: stefano.dossi@polimi.it

[c] F. Maggi
Dept. Aerospace Science and Technology
Politecnico di Milano
Via La Masa 34, 20156 Milano, Italy
E-mail: filippo.maggi@polimi.it

despite the oxide weakening, the chemical process tends to reduce the metal content with a depletion of Al mass fraction of about 4-8% with respect to the virgin powder [15]. Moreover, the impact on environment of aluminum fluoride and other fluorinated derivatives evolved by the combustion of treated particles should be carefully considered. In the second case, mechanical milling (MM) can be used to achieve several results such as creation of amorphous powders, structure change, or production of metal-ceramics composites [16, 17]. Despite the existence of several synthesis techniques, one of the main (common) objectives is to increase the available interface area between powder and oxidizer.

The interest in mechanical activation hails from 1970s when the possibility to produce metals with enhanced physical properties by MM was discovered [16]. During the successive decades, interest in mechanical activation rapidly grew producing several papers on the subject [16]. From a propulsive point of view, mechanical activation is very interesting since it has proven to promote reduction of both initiation temperature and activation energy, thus increasing powder reactivity [18, 19]. Also for MM, a reduction of powder metal content has been observed [20]. This behavior is imputable to the process itself. During mechanical processing particles are stressed and their shape is modified, with consequent breakage of the oxide shell and oxidation of the exposed metal [17, 20]. The amount of lost metal depends on the activation procedure (milling time, environment, etc...). For a simple Al powder alloyed for 3 hours, the metal content loss is in the range of 1-2% making this technique particularly attractive under this point of view [20]. The result in terms of reactivity enhancement, size, and morphology obtainable through a MM process is influenced by several factors such as treatment duration, process control agent (PCA) selection and mass ratio between milling media and powder [21-23]. Depending on the specific intent of the activation, a batch production can require few minutes to some hours [20, 21, 24]. During grinding, cold welding phenomena can take place, inducing the adhesion of particles among themselves, onto the milling media, and onto the jar walls. This phenomenon can be inhibited using an appropriate PCA (e.g. hexane, stearic acid, etc...) [23,25].

In this paper, the production and characterization of several μ Al-metal oxide mixtures activated by MM are presented and discussed. For comparison, the virgin powder and a batch activated by MM without additives are presented too. A detailed characterization comprising SEM analyses, particle size distribution, active metal content, morphology, non-isothermal oxidation at low heating rate, and ignition temperature, is presented to demonstrate the effects of the activation process and of the additives on powder ignition properties. Both low and high heating rate tests are included.

2 Powder activation

Nominally 30 μ m propulsion-grade spherical aluminum (ALPOCO L.t.d, England) was selected as raw material for the mechanical activation. The powder was mixed with several additives, whose specifications are reported in Table 1, into a stainless-steel jar of 125 ml. The reader should be aware that NiO and PbO are dangerous substances according to the European Chemical Agency. Whereas for scientific purposes this risk can be mitigated at lab-scale, an eventual large scale propulsion application should follow a life cycle environmental impact assessment.

Table 1. Metal oxides used for Al activation

Formula	Nominal size, μ m	Purity, %	Bulk density, g/cm ³	Supplier
MoO ₂	< 1.000	99.0	6.95	S-A
Fe ₂ O ₃	0.005	99.3	5.24	MACH-I
NiO	< 0.050	99.8	6.67	S-A
PbO	< 10.000	99.9	9.53	S-A

The activation process was executed in air using a single station centrifugal mill S100 (Retsch GmbH, Germany) at 500 rpm for 30 minutes. A set of 3 mm and 6 mm AISI 304 stainless steel balls were employed with a ball-to-powder mass ratio (BPR) of 5:1. Toluene was selected as PCA to prevent from particle cold welding during the treatment. The produced powders with their respective labels and compositions are listed in Table 2. In addition to the non-activated virgin powder (PW1), four mixtures (PW3 to PW6) were produced adding metal oxides. For completeness, the virgin Al powder was processed without additives using the same treatment described above (PW2).

Table 2. Tested powders and reference labels

Label	Al %	Additive		PCA %
		Id.	%	
PW1 (baseline)	100.0	-	-	-
PW2	100.0	-	-	2.0
PW3	97.5	MoO ₂	2.5	2.0
PW4	97.5	Fe ₂ O ₃	2.5	2.0
PW5	97.5	NiO	2.5	2.0
PW6	97.5	PbO	2.5	2.0

3 Results

3.1. Granulometry

Particle size distribution analyses were carried out through a MASTERSIZER 2000 laser granulometer (Malvern Instruments Ltd, England) using the dry dispersion unit SCIROCCO (post-processed by the machine software, version 5.60). For each ingredient, five tests were executed. The exclusion of outliers is operator independent and is based on the comparison of the residuals, which are quality indicators of the measurements supplied directly by the machine

software. The three results showing the lowest residual values contribute to the final average.

Table 3 presents the particle size distribution. The activation treatment without additives (PW2) causes a consistent increment of both $d(0.5)$ and $D[4,3]$. When oxides are used, the result depends on the additive, although a smaller $D[4,3]$ is observed. Powder PW4 and PW5 exhibit about the same size and are very similar to the baseline. Conversely, the powders PW3 and PW6 show an evident increment of both $d(0,5)$ and $D[4,3]$. It appears that the use of a metal oxide with better dispersion capability (namely, nanometric), tends to hinder the formation of clusters and big particles, strongly containing the growth of the parameter $d(0.9)$. In addition, the finest part of the granulometric curve is preserved, as demonstrated by $d(0.1)$ and $d(0.5)$.

Table 3. Granulometry of tested powders (average of three measurements with 95% t-student confidence interval).

Label	$d(0.1)$, μm	$d(0.5)$, μm	$d(0.9)$, μm	$D[4,3]$, μm
PW1	16.0±0.1	44.7±0.2	99.2±0.8	52.3±0.3
PW2	24.4±3.1	74.3±9.7	217.3±17.5	102.0±9.9
PW3	22.1±1.5	69.7±2.3	219.2±8.3	99.7±2.2
PW4	16.1±0.4	48.8±1.2	118.1±3.2	59.3±1.7
PW5	17.5±2.6	50.2±7.6	127.1±9.7	64.4±5.7
PW6	21.5±0.4	68.3±1.0	165.1±3.2	82.6±1.3

3.2. Microscopy

Powder surface qualitative morphology was analyzed by a TM-3000 tabletop scanning electron microscope (Hitachi High-Tech Ltd, Japan). Figure 1 exhibits the baseline material, while SEM images of samples PW4 and PW6 are shown in Figures 2 and 3, respectively.

The virgin powder PW1 is characterized by rounded (or at most elongated) particles. Small granules exhibit a typical spherical shape, while big particles are less regular. The ball milling process causes a significant morphological variation, evident from Figures 2 and 3. In this case, particles become flat with a relatively rough surface. The presence of an additive tends to reduce the apparent size of the flakes. The additive distribution is generally uniform when the substance is nanometric, as shown in Figure 2 for powder PW4. In the case of micrometric ingredients, metal oxides are not perfectly homogenized with aluminum, resulting in the bright spots visible on the particle surface due to voltage contrast (see Figure 3 for powder PW6). This effect consists of confined enhancement of image contrast and consequent morphology distortion caused by local charge accumulation and non-uniform potential [26,27].

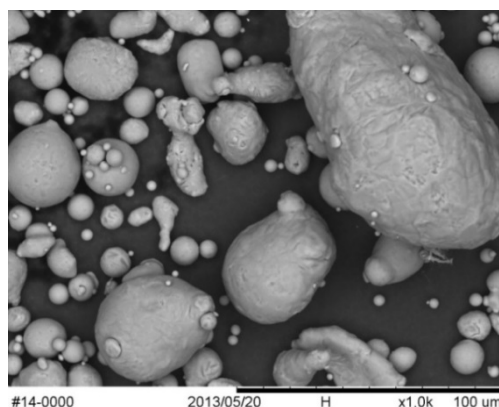


Figure 1. SEM image of the reference powder (PW1) before the activation treatment

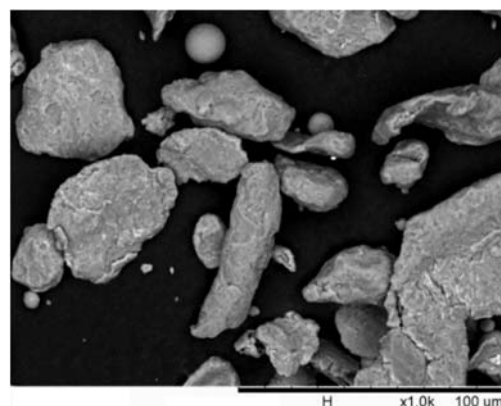


Figure 2. SEM image of the powder processed with 2.5% iron oxide (PW4).

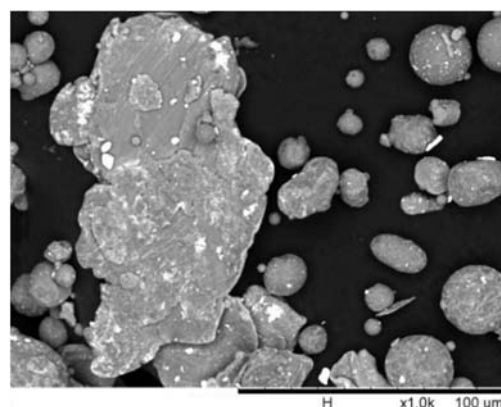
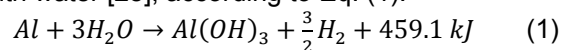


Figure 3. SEM image of the powder processed with 2.5% lead oxide (PW6).

3.3. Metal Content

The active metal content of the samples was measured using the hydrolysis technique. A small amount of powder was dipped into a $\text{H}_2\text{O}/\text{NaOH}$ solution and the evolved hydrogen was monitored through a graduated device. The alkaline solution dissolves the particle oxide layer allowing the reaction of Al with water [28], according to Eq. (1).



Mechanical activation reduces the powder metal content. As shown in Table 4, the sole milling process causes a reduction of the metal content of

about 1-2% due to Al reaction with the oxygen contained in the jar. The addition of a metal oxide is responsible for a further reduction of Al content. Powders PW3 and PW6 contain 2.5% of additive. The active metal content decrease is consistent with the contemporary presence of the additive and the effect of the activation process. In this respect, samples PW4 and PW5 show a metal content lower than expected. The reason is not clear. It is worth noting that both powders contain an additive with nanometric size, instead of micrometric one. Higher milling efficacy may result. Further tests are needed to clarify this aspect.

Table 4. Active metal content of powders (average of four measurements with 95% t-student confidence interval).

Label	Active metal content, %
PW1	99.6 ± 0.1
PW2	97.5 ± 1.0
PW3	96.3 ± 0.7
PW4	93.7 ± 0.8
PW5	93.2 ± 1.0
PW6	95.2 ± 0.8

3.4. Non-Isothermal Oxidation at Low-Heating Rate

Sample behavior at low heating rate was evaluated through simultaneous thermogravimetric-differential thermal analyses (TG-DTA or STA) using an Exstar 6200 (Hitachi – Seiko Ltd., Japan). Samples of 1.75 mg were tested in air (flow rate 150 ml/min) at 10 K/min from ambient temperature to 1370 K, following a standard internal procedure for oxidation testing. Thermogravimetric (TG) and differential-thermal (DTA) traces are reported in Figures 4 and 5.

The reference material, PW1, features a limited reactivity, confirmed by the absence of exothermic peaks during DTA tests and by a poor final mass gain (lower than 10 %), within the range of the TG analyses, limited by apparatus capability. All the other samples exhibit an evident exothermic reaction after Al melting. Samples PW2, PW5, and PW6 feature the highest onset temperature at about 1340 K and the mass gain at the end of the test is approximately 20% for all of them. On the contrary, the powders PW3 and PW4 are characterized by an anticipated exothermic peak, located at about 1260 K, and by a final mass gain of 30.7% and 41.5% respectively.

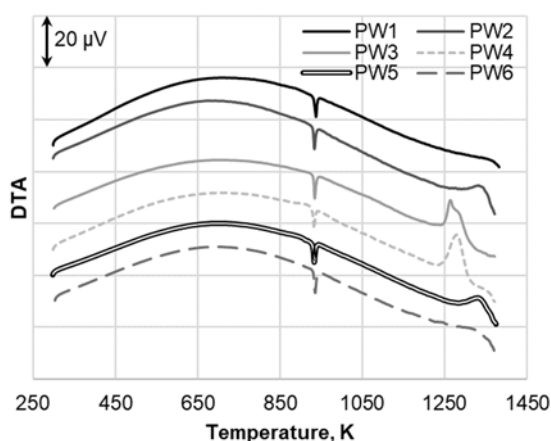


Figure 4. DTA traces for the six tested powders. Curves are shifted for better reading.

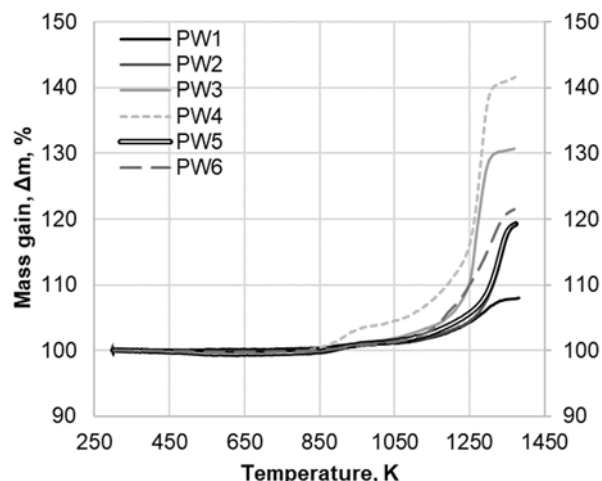


Figure 5. TG traces for all the tested powders

3.5. Ignition Temperature

Ignition temperature was evaluated with a fast heating rate by a hot wire technique. Experimental set up scheme is reported in Figure 6. A heating element (HE), manufactured from a FeCrAl-based alloy wire, was obtained through a procedure of cold forging and has the double function of sample support and heater of the powder at a quasi-constant rate (Figure 7).



Figure 6. CAD model of the heating element used for powder sample ignition tests

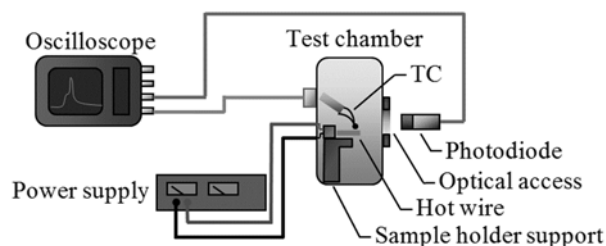


Figure 7. Scheme of the experimental apparatus for fast heating rate tests

Few milligrams of sample were positioned at the center of the forged wire. A thermocouple (TC) was dipped into the powder heap. Then, the system was powered, and the hot wire was heated due to the Joule effect. Signals from the TC and from a photodiode (PD) observing the process were sent to a four-channel oscilloscope. Tests can be executed at different pressures and in several oxidizing environments depending on the specific needs. In this work, experiments were carried out in air at ambient

pressure and 300 K/s (max temperature: 1200 K). Recorded signals were post-processed identifying the ignition temperature by a rapid change of the TC curve slope, confirmed by the PD. Inconsistent data (e.g. those characterized by heating rate exceeding limits or by staggered PD/TC ignition instants) were immediately rejected, while other experimental outcomes were analyzed through the Chauvenet's statistical criterion to assess the presence of outliers [29]. Ignition temperature (T_{ign}) results are reported in Table 5.

Table 5. Ignition temperature in air at ambient pressure. Uncertainty is computed assuming a t-student distribution with 95% of confidence level.

Label	Ignition	T_{ign} , K	Uncertainty, %
PW1	No ^a	N.Av.	N.Av.
PW2	No ^a	N.Av.	N.Av.
PW3	Yes	904.0 ± 14.8	1.64
PW4	Yes	876.4 ± 12.8	1.46
PW5	Yes	922.6 ± 17.0	1.82
PW6	Yes	905.5 ± 15.2	1.67

^a) Beyond experimental capability (about 1200 K)

Under the tested experimental conditions, no ignition can be observed for both PW1 and PW2, showing that the sole milling treatment employed in this work is not enough to adequately increase powder reactivity. Conversely, metal oxides play a key role in reducing the ignition temperature, probably promoting local metal-oxide reactions (e.g. thermite reactions), capable of triggering particle ignition. All the samples activated with additives feature an ignition temperature lower than the Al melting point. In this respect, the best results are shown by the powders PW3, PW4 and PW6, respectively doped with MoO₂, Fe₂O₃ and PbO, while the highest T_{ign} among the additive-based ingredients is shown by the powder PW5 containing NiO.

4 Discussion

The proposed characterization methodologies capture some of the most significant effects that mechanical activation has on the powder features. All the processed materials feature a peculiar flake-like shape with a relatively rough surface. The presence of white spots, evidence of a non-perfect homogenization between additive and metal, has been detected only for particles activated with micrometric metal oxides. Granulometric tests revealed a general increment of activated particle size. This effect is particularly evident for activation without additives or with micrometric metal oxides favoring particle aggregation as shown by the high values of $d(0.9)$. On the contrary, nanometric substances tend to hinder cold cohesion effects. In this respect, it is important to notice that laser-based granulometric analyses are optimized for spherical powders. An even more detailed characterization would require the coupling of standard granulometric data with information data sets on statistically representative shape and surface finishing descriptors, which are beyond the scope of this work. Reactivity enhancement of activated powders has been confirmed at low heating rate for all the activated

materials and, in particular, for the samples PW3 and PW4. With the sole exception of the baseline, all the powders exhibit an evident exothermic peak and a peculiar mass gain above 1200 K, close to the upper end of the test range. The situation changes at high heating rate. Ignition temperature, if detected, is always below the melting point of Al and it is confirmed only for doped powders, testifying the key role played by the additive in the ignition process as well as the importance of the heating rate. This fact is more evident considering that the powder PW2, milled without additives, features a visible reaction during low-heating rate tests, but does not ignite at high heating rate.

The specific ball milling treatment used in this work is responsible for a generalized reduction of the powder metal content, with a more marked depletion when additives are used. The final metal content is not directly related to the sample reactivity at low or high heating rate and the use of nanometric metal oxides tends to worsen it, contemporary enhancing powder reaction capability.

5 Conclusion

This paper focused on the mechanical activation of micrometric aluminum powders and in the characterization of their energetic features. A propulsion-grade μAl with 30 μm spherical particles has been selected as raw material. This powder has been mechanically activated through a ball milling process with and without additives. Activation parameters were always uniformly applied across the different batches considered in the work. Five powders (four with metal oxides and one without additives) were produced through a centrifugal mill (30 minutes at 500 rpm in air) and then characterized in terms of particle size distribution, qualitative morphology, metal content, low heating rate non-isothermal oxidation and ignition temperature.

Activated materials feature a general irregular shape independently on the use of metal oxides. As pointed out by SEM images, micrometric additives are difficult to disperse resulting in white spots located on activated particle surface. On the contrary, the phenomenon has not been detected with nanometric substances. The ball milling process causes a depletion of the metal content due to particle oxidation during the treatment. The presence of an additive causes a further reduction of the active aluminum content, from about 2% up to 7%. The analyses evidenced a potential influence of the additive granulometry on metal content reduction (from 3%-4% for micron-sized materials to about 7% for nanometric substances). Despite a moderate reduction of the active aluminum content, enhancement of powder reactivity has been observed both at low and high heating rate. Despite the general reactivity improvement observed during TG/DT analyses, the sample activated without additives did not ignite during fast-heating tests, thus confirming the key role played by the selected metal oxides.

Milling treatment with additives produced highly reactive powders leading to a strong reduction of ignition temperature. This result, together with the relatively high metal content, make this kind of ingredients very appealing for further experimentations in solid propellants to evaluate their effects on both burning rate and condensed combustion product size.

Symbols and Abbreviations

D[4,3]	Mass mean diameter
d(0.1)	diameter of the 10 th percentile
d(0.5)	diameter of the 50 th percentile
d(0.9)	diameter of the 90 th percentile
T _{ign}	Ignition temperature
μAl	Micrometric aluminum
aAl	Activated aluminum
CCP	Condensed combustion products
DTA	Differential thermal analysis
HE	Heating element
MM	Mechanical milling
nAl	Nanoaluminum
PDA	Process control agent
PD	Photodiode
S-A	Sigma Aldrich
SEM	Scanning electron microscope
SP	Solid propellant
SRM	Solid rocket motor
STA	Simultaneous thermal analysis
TC	Thermocouple
TG	Thermogravimetry

Acknowledgements

The authors acknowledge the valuable work of Mr. Luca Facciolati, performed during his thesis work.

References

- [1] E. W. Price, R. K. Sigman, J. K. Sambamurthi, C. J. Park, *Behavior of Aluminum in Solid Propellant Combustion*, Scientific Report, DTIC Accession Number ADA118128, Georgia Institute of Technology, Atlanta, GA, USA, **1982**.
- [2] D. Reydellet, *Performance of Rocket Motors with Metallized Propellants*, Advisory Report AR-230, AGARD, Neuilly sur Seine, FR, **1986**.
- [3] L. Meda, G. Marra, L. Galfetti, F. Severini, L. T. De Luca, Nano-aluminum as Energetic Material for Rocket Propellants, *Mat. Sci. Eng. C* **2007**, 27, 1393-1396.
- [4] L. T. De Luca, L. Galfetti, F. Severini, L. Meda, G. A. Marra, A. B. Vorozhtsov, V. S. Sedoi, V. A. Babuk, Burning of Nano-aluminized Composite Rocket Propellants, *Combust. Explos. Shock Waves* **2005**, 41, 680-692.
- [5] L.T. De Luca, L. Galfetti, G. Colombo, F. Maggi, A. Bandera, V. A. Babuk, and V. P. Sinditski, Microstructure Effects in Solid Rocket Propellants, *J. Propul. Power* **2010**, 26, 724-733.
- [6] F. Maggi, A. Bandera, L. Galfetti, L. T. De Luca, T. L. Jackson, Efficient Solid Rocket Propulsion for Access to Space, *Acta Astronaut.* **2010**, 66, 1563-1573.
- [7] F. Maggi, S. Dossi, C. Paravan, S. Carlotti, L. Galfetti, Role of Pressure and Aluminum Size in Solid Propellant CCP Generation, *53rd AIAA/SAE/ASEE Joint Propulsion Conference*, Atlanta, GA, USA, July 10-12, **2017**, AIAA Paper No.2017-5076.
- [8] S. Dossi, A. Reina, F. Maggi, L.T. De Luca, Innovative Metal Fuels for Solid Rocket Propulsion, *Int. J. Energetic Materials Chem. Prop.* **2012**, 11, 299-322.
- [9] A. A. Gromov, Y. I. Strokova, U. Teipel, Stabilization of Metal Nanoparticles – A Chemical Approach, *Chem. Eng. Technol.* **2009**, 32, 1049-1060.
- [10] C. Paravan, F. Maggi, S. Dossi, G. Marra, G. Colombo L. Galfetti, Pre-burning Characterization of Nanosized Aluminum in Condensed Energetic Systems, in: *Energetic Nanomaterials* (Eds.: V. E. Zarko, A. A. Gromov) Elsevier, Amsterdam, NL, **2016**, pp. 341-368.
- [11] E. W. Dreizin, Metal-based reactive nanomaterials, *Prog. Ener. Combust.* **2009**, 35, 141-167.
- [12] A. A. Gromov, E. M. Popenko, Yu. Yu Shamina, A. V. Sergienko, A. P. Ilyin, N. I. Popok, Effect of addition of ultrafine powders on the rheological properties and burning rate of energetic condensed systems, *Combust. Explos. Shock Waves* **2007**, 43, 46-50.
- [13] S. Dossi, *Mechanically activated aluminum fuels for high-performance solid rocket propellants*, PhD Thesis, Politecnico di Milano, Milan, IT, **2014**.
- [14] A. Hahama, A. Gany, K. Palovuori, Combustion of activated aluminum, *Combust. Flame* **2006**, 145, 464-480.
- [15] F. Maggi, S. Dossi, C. Paravan, L. T. De Luca, M. Liljedahl, Activated aluminum powders for space propulsion, *Powder Technol.* **2015**, 270, 46-52.
- [16] D. L. Zhang, Processing of advanced materials using high-energy mechanical milling, *Prog. Mater. Sci.* **2004**, 49, 537-560.
- [17] C. C. Koch, J. D. Whittenberger, Review mechanical milling / alloying of intermetallics, *Intermetallics* **1995**, 4, 339-355.
- [18] V. Yu. Filimonova, M. A. Korchagin, V. V. Evstigneev, Anomalous Decrease in the Activation

Energy and Initiation Temperature of a Thermal Explosion in the Mechanically Activated Composition 3Ni + Al, *Dokl. Phys.* **2009**, 56, 277-280.

Received: ((will be filled in by the editorial staff))
Revised: ((will be filled in by the editorial staff))

- [19] A. S. Shteinberg, Ya-Cheng Lin, S. F. Son, A. S. Mukasyan, Kinetic of high temperature reaction in Ni-Al system: influence of mechanical activation, *J. Phys. Chem. A.* **2010**, 114, 6111-6116.
- [20] P. S. Gilman, W. D. Nix, The structure and properties of aluminium alloys produced by mechanical alloying: powder processing and resultant powder structures, *Metal. Trans. A.* **1981**, 12, 813-824.
- [21] M. Schoenitz, T. S. Ward, E. L. Dreizin, Fully dense nano-composite energetic powders prepared by arrested ball milling, *Proc. Combust. Inst.* **2005**, 20, 2071-2078.
- [22] S. M. Zebarjad, S. A. Sajjadi, Microstructure evaluation of Al-Al₂O₃ composite produced by mechanical alloying method. *Mater. Design* **2006**, 27, 684-688.
- [23] L. M. Shaw, Zawrah, J. Villegas, H. Luo, D. Miracle, Effects of process control agents on mechanical alloying of nanostructured aluminum alloys. *Metal. Trans. A.* **2003**, 34, 159-170.
- [24] S. M. Umbrajkar, M. Schoenitz, E. L. Dreizin, Exothermic reactions in Al-CuO nanocomposites. *Thermochim. Acta* **2006**, 451, 34-43.
- [25] R. H. Chen, C. Suryanarayana, M. Chaos, Combustion characteristics of mechanically alloyed ultrafine-grained Al-Mg powders, *Adv. Eng. Mater.* **2008**, 8, 563-567.
- [26] D.A. Moncriefft, V.N.E. Robinson and L.B. Harris, Charge neutralisation of insulating surfaces in the SEM by gas ionization, *J. Phys. D: Appl. Phys.* **1978**, 11, 2315-2325.
- [27] A.E. Vladár and M.T. Postek, The scanning Electron Microscope, in: *Handbook of Charged Particle Optics*, Second Edition (Ed. J. Orloff), CRC Press, Boca Raton, FL, USA, 2008, pp. 437-496.
- [28] A. P. Astankova, A. Yu. Godymchuk, A. A. Gromov, A. P. Il'in, The kinetics of self-heating in the reaction between aluminum nanopowder and liquid water, *Russ. J. Phys. Ch.* **2008**, 82, 1913-1920.
- [29] J.R. Taylor, Rejection of data, in: *An Introduction to Error Analysis*, chapter 6, second edition, University Science Books, Sausalito, CA, USA, 1997, pp. 165-172.

